

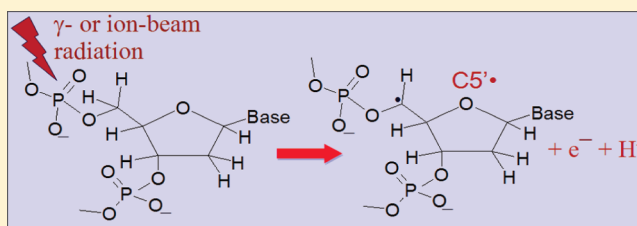
Direct Formation of the C5'-Radical in the Sugar–Phosphate Backbone of DNA by High-Energy Radiation

Amitava Adhikary, David Becker, Brian J. Palmer, Alicia N. Heizer, and Michael D. Sevilla*

Department of Chemistry, Oakland University, Rochester, Michigan 48309, United States

S Supporting Information

ABSTRACT: Neutral sugar radicals formed in DNA sugar–phosphate backbone are well-established as precursors of biologically important damage such as DNA strand scission and cross-linking. In this work, we present electron spin resonance (ESR) evidence showing that the sugar radical at C5' (C5'•) is one of the most abundant (ca. 30%) sugar radicals formed by γ - and Ar ion-beam irradiated hydrated DNA samples. Taking dimethyl phosphate as a model of sugar–phosphate backbone, ESR and theoretical (DFT) studies of γ -irradiated dimethyl phosphate were carried out. $\text{CH}_3\text{OP}(\text{O}_2^-)\text{OCH}_2^\bullet$ is formed via deprotonation from the methyl group of directly ionized dimethyl phosphate at 77 K. The formation of $\text{CH}_3\text{OP}(\text{O}_2^-)\text{OCH}_2^\bullet$ is independent of dimethyl phosphate concentration (neat or in aqueous solution) or pH. ESR spectra of C5'• found in DNA and of $\text{CH}_3\text{OP}(\text{O}_2^-)\text{OCH}_2^\bullet$ do not show an observable β -phosphorus hyperfine coupling (HFC). Furthermore, C5'• found in DNA does not show a significant C4'-H β -proton HFC. Applying the DFT/B3LYP/6-31G(d) method, a study of conformational dependence of the phosphorus HFC in $\text{CH}_3\text{OP}(\text{O}_2^-)\text{OCH}_2^\bullet$ shows that in its minimum energy conformation, $\text{CH}_3\text{OP}(\text{O}_2^-)\text{OCH}_2^\bullet$, has a negligible β -phosphorus HFC. On the basis of these results, the formation of radiation-induced C5'• is proposed to occur via a very rapid deprotonation from the directly ionized sugar–phosphate backbone, and the rate of this deprotonation must be faster than that of energetically downhill transfer of the unpaired spin (hole) from ionized sugar–phosphate backbone to the DNA bases. Moreover, C5'• in irradiated DNA is found to be in a conformation that does not exhibit β -proton or β -phosphorus HFCs.



INTRODUCTION

DNA strand breaks (especially the double strand break) are the main cause for radiation-induced cell death, mutation, aging, and carcinogenesis.^{1–3} Neutral sugar radicals, such as the C5' sugar radical (C5'•), formed in the sugar–phosphate backbone, are precursors of immediate (i.e., frank) DNA strand breaks.^{1–3} The nucleoside 5'-aldehyde, formed from C5'•, was recently shown to be a major product of oxidation of DNA in solution and in cells.⁴ Numerous evidence of the formation of radiation-induced stable DNA damage products via intramolecular C5'–C8 cycloaddition⁵ and other C5'–radical-induced adduct radicals including interstrand cross-linking⁶ and DNA–protein cross-linking¹ have been reported in the literature. We note that apart from strand breaks, cross-links represent more complex DNA lesions than simple base damage (e.g., dihydrothymidine, 8-oxo-guanine, etc.). The formation of a number of strand breaks as well as cross-links within a very close proximity (e.g., within 10 base pairs) leads to the production of a multiply damaged site (MDS), which disrupts the helical rigidity of DNA.^{1,2,5–7} As a result, MDS is a potentially lethal lesion that is difficult to repair.^{1,2} Once formed, C5'• can undergo three competitive reactions: strand break formation at the 5'-site, cross-link production, and cyclization.

To date, two mechanisms of neutral sugar radical formation via direct ionizations of high energy radiations (e.g., such as γ -radiation, X-rays, and ion beams) have been proposed as

follows: (a) deprotonation of the directly ionized sugar–phosphate backbone^{8–13} and (b) deprotonation of the excited purine (guanine and adenine) cation radicals.^{8–10} The best overall estimate of the probability of direct ionization at a given site in DNA, such as the sugar, phosphate, or DNA base, is provided by the number of valence electrons at that site.^{8,9} For DNA, from the number of valence electrons alone, ca. 43% ionizations should initially occur at the bases and the remainder at the sugar–phosphate moiety.^{8,9,10a} Contrary to these expectations, electron spin resonance (ESR) studies of trapped DNA radicals at 77 K show that transfer of a hole (unpaired spin due to electron loss) from the sugar–phosphate moiety to the base increases the extent of trapped holes on the bases to ca. 77%.^{8–13} The remaining holes in the sugar–phosphate backbone that are not transferred to the base are fixed by deprotonation and, hence, are found as neutral carbon-centered sugar radicals, for example, C5'•.^{8–13} Similar conclusions were obtained via quantification of base release and base damage products that were formed because of the holes at bases and at the sugar–phosphate backbone in irradiated DNA.^{14,15} On the basis of number of valence electrons of the phosphate group alone, it can be estimated that nearly half of all ionization events

Received: March 12, 2012

Revised: May 1, 2012

Published: May 3, 2012

taking place on the sugar–phosphate backbone should occur at the phosphate moiety. Yet, ESR spectra of γ -irradiated hydrated high molecular weight salmon testes DNA recorded at 77 K show that only insignificant amounts (ca. 0.01%) of phosphate radicals are formed in these samples.^{9,10a,16} In the case of ion-beam-irradiated DNA,^{17,18} ESR spectra of phosphate radicals were reported in very small abundance (less than 0.1%) but were associated with dissociative electron attachment (DEA) via attack of low-energy electrons (LEEs)^{8–10,16–18} and not a result of one-electron oxidation of the sugar–phosphate backbone via direct ionization.

Radiation-induced ionization of the monoanionic phosphate group has been theoretically modeled. One-electron oxidation of the monoanionic phosphate group in 5'-TMP in aqueous media was predicted theoretically by LeBreton and co-workers using the DFT/SCF/3-21G method.¹⁹ Furthermore, in the gas phase and employing the DFT/B3LYP/DZP++ method that is suitable for anionic species, Hou et al.²⁰ and Close²¹ show that one-electron oxidation of 2'-deoxyadenosine-5'-monophosphate (5'-dAMP) monoanion leads to localization of considerable spin density on the phosphate. However, the work of Close²¹ points out that using the DFT/B3LYP/6-31G(d) method, results similar to those reported by Hou et al.²⁰ could be obtained with the same level of accuracy, but the mixing of the highest occupied molecular orbital (HOMO) with the HOMO-1 as found in the work of Hou et al. was avoided.²⁰ However, ESR studies carried out at 10 K on X-irradiated single crystals of nucleotides, for example, 5'-dGMP,²² as well as on γ -irradiated aqueous glassy solutions of 5'-dAMP at 77 K,²³ and on photoionized (via biphotonic ionization caused by 248 nm laser at 77 K) aqueous glassy solutions of 5'-dCMP at 77 K²⁴ show no evidence of phosphate radical formation. In every situation, carbon-centered radical(s) were produced without any observable β -phosphorus coupling. Furthermore, γ -irradiated diethyl phosphoric acid salts also showed the formation of no phosphate radicals but show the $\text{CH}_3\text{C}(\bullet)\text{-HOPO}_2\text{OCH}_2\text{CH}_3$ and the ethyl radical.^{25a,b} Moreover, ESR studies of γ -irradiated monoalkyl phosphates^{25c} as well as of X-ray-irradiated hydroxyalkyl phosphates^{25d}—for example, α -D-glucose-1-phosphate, D-glucose-6-phosphate, D-ribose-5-phosphate, and β -glycerol phosphate—provide no evidence for phosphate radical formation at 77 K. Similar to the nucleotides, the formation of carbon-centered radicals without any observable β -phosphorous coupling was observed in these hydroxyalkyl phosphates at 77 K. Moreover, the C5'-radical-induced cyclic product (for example, 5',6-cyclo-5,6-dihydrothymidine) has been isolated as a significant product in frozen (196 K) aqueous solutions of thymidine,^{25e} 2'-deoxycytidine,^{25f} and 2'-deoxyuridine,^{25e} after γ -irradiation at 196 K.

In this work, we seek to understand the mechanism of direct ionization events on the phosphate moiety of the DNA–sugar–phosphate backbone. Direct one-electron ionization of hydrated salmon sperm DNA samples by γ - and ion-beam irradiation at 77 K has been investigated using ESR spectroscopic studies at 77 K. Furthermore, ESR studies and density functional theory (DFT) calculations were employed to study the dimethyl phosphate anion as a model system for the phosphate portion of DNA. The main aim of this work is to elucidate the likely mechanisms of formation of sugar radicals formed by direct ionization of the sugar–phosphate backbone by γ - and ion-beam-irradiated DNA. We find results that suggest that the formation of neutral C5^\bullet after phosphate ionization involves a rapid deprotonation from the $\text{C5}'$; the

formation of C5^\bullet occurs in a specific conformation that has little β phosphorus or $\text{C4}'\text{-H}$ β -proton coupling.

MATERIALS AND METHODS

Compounds. Lithium chloride (99% anhydrous, Sigma Ultra) and Salmon testes DNA (sodium salt, 57.3% AT, and 42.3% GC) were purchased from Sigma Chemical Company (St. Louis, MO). Potassium persulfate (crystal) was obtained from Mallinckrodt, Inc. (Paris, KY). Deuterium oxide (99.9 atom % D), potassium ferrocyanide ($\text{K}_4[\text{Fe}(\text{CN})_6]$), and potassium ferricyanide ($\text{K}_3[\text{Fe}(\text{CN})_6]$) were obtained from Aldrich Chemical Co. Inc. (Milwaukee, WI). Dimethyl phosphate was procured from Pfaltz & Bauer (Waterbury, CT). Following our earlier work,^{26–35} all compounds were used without any further purification.

Sample Preparation and Their Storage. *a. Dimethyl Phosphate.* Neat dimethyl phosphate (1 mL) was used. Also, following our previous work with the monomers of DNA and RNA,^{27–35} 5–10 mg of dimethyl phosphate was dissolved in 1 mL of 7.5 M LiCl in D_2O and ca. 8–10 mg of $\text{K}_2\text{S}_2\text{O}_8$ was added as an electron scavenger.

b. pH Adjustments of Dimethyl Phosphate Solutions. Following our work,^{30–35} by quickly adding the appropriate micromole amounts of 0.1–1 M NaOH in D_2O , the pH values of the solutions of dimethyl phosphate were adjusted at ca. 8 and at ca. 12 under ice-cooled conditions. Because of the high ionic strength (7.5 M LiCl) of these solutions and also because of the use of pH papers, all of the pH values reported in this work are approximate.^{30–35} These homogeneous solutions were degassed by bubbling thoroughly with the nitrogen gas at room temperature.

c. Preparation of Dimethyl Phosphate Samples. The neat dimethyl phosphate as well as the pH-adjusted homogeneous solutions of dimethyl phosphate were drawn into 4 mm Suprasil quartz tubes (Catalog no. 734-PQ-8, WILMAD Glass Co., Inc., Buena, NJ). The tubes containing these solutions were rapidly immersed into liquid nitrogen (77 K) so that rapid cooling of solutions containing 7.5 M LiCl to 77 K resulted in transparent glassy solutions.

d. Preparation of DNA Pellets. Homogeneous solutions of DNA (100 mg/mL) in the presence of both $\text{K}_3[\text{Fe}(\text{CN})_6]$ (electron scavenger) and $\text{K}_4[\text{Fe}(\text{CN})_6]$ (hole scavenger), with a 1:20 mol ratio of scavenger to base pair, were prepared in the absence of oxygen. These DNA samples were lyophilized and then rehydrated in D_2O (hydration $\Gamma = 12 \pm 2 \text{ D}_2\text{O}/\text{nucleotide}$) by following the procedure delineated in ref 16.

These hydrated DNA samples having both $\text{K}_3[\text{Fe}(\text{CN})_6]$ and $\text{K}_4[\text{Fe}(\text{CN})_6]$ were then pressed into cylinders, that is, pellets (0.4 cm by 1 cm height) in a glovebag under nitrogen atmosphere using a Teflon-coated aluminum dye and press and were immediately placed in liquid nitrogen in the dark.^{16–18,26} Before and after irradiation, all samples were stored in Teflon containers at 77 K in the dark.

Irradiation of Samples and Storage of the Irradiated Samples. *a. γ -Irradiation of Glassy Samples.* Following our previous work,³⁵ the neat dimethyl phosphate as well as the pH-adjusted homogeneous glassy (7.5 M LiCl/ D_2O) solutions of dimethyl phosphate samples were γ -irradiated (absorbed dose = 1.4 kGy) at 77 K in Teflon containers.

b. Ion-Beam Irradiation of DNA Pellets. Following the procedure mentioned in ref 18, the hydrated DNA pellets having both $\text{K}_3[\text{Fe}(\text{CN})_6]$ and $\text{K}_4[\text{Fe}(\text{CN})_6]$ were irradiated at 77 K at the National Superconducting Cyclotron Laboratory

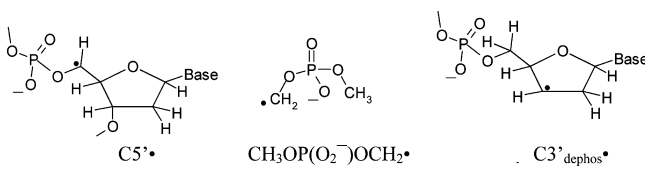
(NSCL) at Michigan State University. Argon-40 beams with specific energy of 100 MeV/nucleon were used for the irradiation. Employing the ion-beam dosimetry mentioned in ref 18, the absorbed dose of the DNA pellet was found to be 20 kGy. The irradiated glassy samples of the monomers and the DNA pellets were stored in Teflon containers at 77 K in the dark for subsequent studies.

Annealing of the Glassy Samples. As per our earlier work³⁵ γ -irradiated (dose = 1.4 kGy) glassy samples of dimethyl phosphate were progressively annealed from 140 to 160 K in 5 °C steps for 15–20 min at each temperature. Employing a variable temperature assembly (Air products), annealing of each sample was carried out in the dark via cooled nitrogen gas, which regulated the gas temperature within ± 4 °C. Annealing the sample softens the glass, allowing the matrix radical, $\text{Cl}_2^{\bullet-}$, to migrate and react by one-electron oxidation of the solute.³⁵

Theoretical Calculations. DFT calculations were performed with the Spartan'10 program set.^{36a} Structures were optimized employing the B3LYP/6-31G(d) approach. HFCCs were computed using the Gaussian 09 suite of programs.^{36b} We note here that the B3LYP/6-31G(d) level has been found to give accurate predictions of structures, spin densities, and hyperfine coupling constant (HFCC) values.^{10,11,13,30–32,34,37–39}

ESR. ESR spectra were recorded using a Varian Century Series ESR spectrometer operating at 9.3 GHz with an E-4531 dual cavity, 9 in. magnet, and with a 200 mW klystron.^{26–35} Fremy's salt, $g(\text{center}) = 2.0056$, $A_N = 13.09$ G, was used for field calibration.³² Following γ -irradiation without or followed by annealing, the neat and glassy samples of dimethyl phosphate were immersed immediately in liquid nitrogen (77 K), and an ESR spectrum was recorded at 40 dB (20 μW). The ESR spectra of the ion-beam-irradiated DNA pellets were recorded at 45 dB (6.3 μW). All ESR spectra are recorded at 77 K. Following our work,³¹ the anisotropic simulations to fit experimentally recorded ESR spectra were carried out with WIN-EPR and SimFonia (Bruker) programs. The structures of the radicals studied in this work are shown in Scheme 1.

Scheme 1. Structures of C5^{\bullet} and $\text{C3'}_{\text{dephos}}^{\bullet}$ Found in DNA as Well as of $\text{CH}_3\text{OP}(\text{O}_2^-)\text{OCH}_2^{\bullet}$ Found in Dimethyl Phosphate Are Shown Here



RESULTS AND DISCUSSION

I. C5^{\bullet} Formation in DNA by Low-LET (γ -Irradiation) and High LET (Ion-Beam Irradiation). In this work, Ar^{18+} ion-beam-irradiated high molecular weight hydrated DNA pellets prepared with $\text{K}_3[\text{Fe}(\text{CN})_6]$ (1/20 bp) as a electron or anion radical scavenger and with $\text{K}_4[\text{Fe}(\text{CN})_6]$ (1/20 bp) as a hole or cation radical scavenger at 77 K have been investigated to test for ESR evidence for C5^{\bullet} (Scheme 1) and other sugar radical formation. These results are compared with similarly prepared and γ -irradiated DNA samples (data taken from ref 16).

In Figure 1A, the ESR spectrum obtained from Ar^{18+} ion-beam (100 MeV/nucleon)-irradiated DNA pellets is shown. In

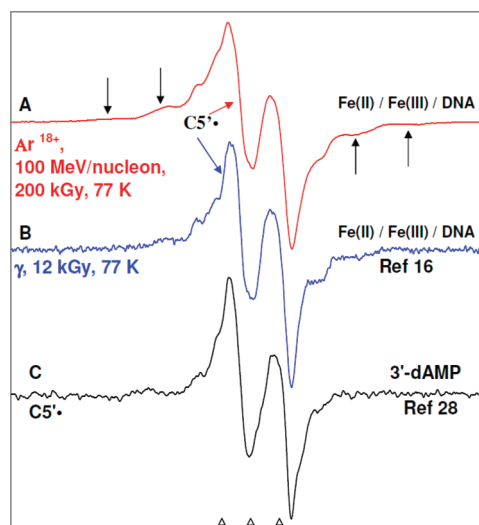


Figure 1. ESR spectra: (A) Ar^{18+} ion-beam (100 MeV/nucleon) irradiated DNA pellets (this work). (B) γ -Irradiated DNA pellets (see ref 16). The irradiations were carried out at 77 K in the presence of both $\text{K}_3[\text{Fe}(\text{CN})_6]$ (electron scavenger) and $\text{K}_4[\text{Fe}(\text{CN})_6]$ (hole scavenger) added at a ratio of (1/20 bp) for each. (C) The established C5^{\bullet} (Scheme 1) spectrum, obtained via photoexcitation of $\text{A}^{\bullet+}$ in the glassy (7.5 M $\text{LiCl}/\text{D}_2\text{O}$) sample of 3'-dAMP.²⁸ The central anisotropic doublet in spectra 1A and 1B is assigned to C5^{\bullet} . In spectra 1A and 1B, the outer line components (indicated by arrows) due to $\text{C3'}_{\text{dephos}}^{\bullet}$ (Scheme 1) are also observed.

Figure 1B, the ESR spectrum obtained from γ -irradiated DNA pellets (dose 12 kGy) at 77 K is shown (from ref 16). Employing benchmark spectra of one-electron oxidized guanine in oligomers,^{9,10,33} of $\text{T}^{\bullet-}$,^{8–13,26} of $\text{C}^{\bullet-}$ [or $\text{C}(\text{N}_3\text{H})^{\bullet}$],^{8–13,26} and of the composite sugar radical spectra^{9,10,16–18,26} the spectra in Figure 1A,B have been analyzed. The analyses suggest that except for a small amount (ca. 5–10%) of $\text{C}(\text{N}_3\text{H})^{\bullet}$, almost all radiation-induced DNA cation and anion radicals are scavenged, and the spectra in Figure 1A,B are due to the composite sugar radical spectrum, which is composed of radicals formed in the sugar–phosphate backbone.

To confirm that the central anisotropic doublet in spectra in Figure 1A,B is due to C5^{\bullet} , that is, due to an anisotropic $\alpha\text{-H}$ (C5'-H) hyperfine coupling, it is compared to an established anisotropic doublet C5^{\bullet} spectrum [anisotropic $\alpha\text{-H}$ (C5'-H) = ca. 21 G, black, Figure 1C] obtained via photoexcitation of adenine cation radical ($\text{A}^{\bullet+}$) in the glassy (7.5 M $\text{LiCl}/\text{D}_2\text{O}$) sample of 3'-dAMP at pH ca. 5²⁸ shown in Figure 1C. Because of the similarities (total hyperfine splitting, line shape, and the g value at the center) of the central anisotropic doublet shown in Figure 1A,B with the established anisotropic doublet C5^{\bullet} spectrum in Figure 1C, the central anisotropic doublet found in Figure 1A,B is assigned to C5^{\bullet} . Analyses of the spectrum in Figure 1A employing the spectrum in Figure 1C as a benchmark of C5^{\bullet} suggests that the ion-beam-irradiated DNA sample has a substantial extent (ca. $25 \pm 10\%$) of C5^{\bullet} present in the spectrum in Figure 1A. Similarly, analyses of the spectrum in Figure 1B employing the spectrum in Figure 1C as a benchmark of C5^{\bullet} suggests that the γ -irradiated DNA sample has even more extent (ca. $40 \pm 10\%$) of C5^{\bullet} present in the composite spectrum sugar–phosphate backbone radicals. Here,

we have used an authentic $C5^{\bullet}$ spectrum derived from the model compounds that has been assigned to $C5^{\bullet}$ based on our work using selective deuteration in the sugar moiety^{8–10,27,32} and using ^{13}C isotope-substituted dAdo at 5'-site in the sugar.²⁸ We note here that we have updated the analyses of $C5^{\bullet}$ of our previous work¹⁶ that had previously suggested that about 30% of $C5^{\bullet}$ was present in the composite spectrum in Figure 1B due to various sugar radicals found in γ -irradiated DNA with Fe(II)/Fe(III). Apart from $C5^{\bullet}$, other prominent line components (indicated by arrows) due to $C3'_{\text{dephos}}^{\bullet}$ [i.e., neutral $C3^{\bullet}$ formed by reductive loss of the 3'-phosphate (Scheme 1)]^{16–18} are also observed in the spectra in Figure 1A,B. $C3'_{\text{dephos}}^{\bullet}$ was associated with DEA via attack of LEEs^{8–10,16–18} and not a result of one-electron oxidation of the sugar–phosphate backbone via direct ionization.

We note here that ESR/ENDOR studies of $C5^{\bullet}$ found in X-ray-irradiated single crystals of dAdo·H₂O^{40,41} as well as of 5'-dGMP·4H₂O²² show one α H anisotropic coupling due to $C5'$ -H atom with its A_{iso} value ranging between 15 and 20 G along with a small A_{iso} value ranging between 2²² and 6 G⁴⁰ from the $C4'$ - β H. The small A_{iso} HFCC value of $C4'$ - β H results in the nucleoside (dAdo) and -tide (5'-dGMP) from a conformation that places the β -hydrogen in a conformation of low HFCC, that is, with a torsion angle of near 70° between the z-axis of the $C5'$ -radical p-orbital and the H-C4' bond. Thus, in this $C5'$ -radical conformation, the $C4'$ -H atom is near the nodal plane of the $C5'$ -radical p-orbital so that a small hyperfine coupling of $C4'$ - β H is observed.^{28,41} For $C5^{\bullet}$ observed after photoexcitation of A^{*+} in an aqueous glass (7.5 M LiCl/D₂O) sample of RNA nucleotide 3'-AMP at pH ca. 6, a very small $C4'$ - β H HFCC value is apparent.³² Yet, at ca. pH 9 where the phosphate group is a dianion and an internal hydrogen bond is formed with OS', the torsion angle between the z-axis of the $C5'$ -radical p-orbital and the H-C4' bond becomes 36°, and this results in a considerable $C4'$ - β H HFCC value of 34.5 G.³² The ESR spectrum showing the anisotropic doublet (ca. 21 G, due to $C5'$ - α H coupling) due to $C5^{\bullet}$ found in high molecular weight DNA (Figure 1A,B) shows no apparent coupling from the $C4'$ - β H. However, we note that small line components in Figure 1C are suggestive of small contributions from other conformations where the $C4'$ - β H HFCC is significant. In fact, the ESR/ENDOR studies of $C5^{\bullet}$ in X-ray-irradiated single crystal of 5'-dGMP·4H₂O reports about four different conformations of $C5^{\bullet}$ arising due to the variation of torsion angle between the z-axis of the $C5'$ -radical p-orbital and the H-C4' bond.²² Moreover, using the DFT/B3LYP/3-21G basis set, the optimized geometry of $C5^{\bullet}$ radical in a B-DNA conformation is shown to be near planar,⁴³ and the torsion angle between the z-axis of the $C5'$ -radical p-orbital and the H-C4' bond is calculated to be 75–80°.⁴² This is supported by our work regarding unequivocal assignment of $C5^{\bullet}$ in 5'-[^{13}C]-dAdo where the HFCC values of $^{13}C5'$ for $C5^{\bullet}$ were calculated using the DFT/B3LYP/6-31G(d) method for both planar and nonplanar conformations of $C5^{\bullet}$ and the theoretically predicted HFCC values (15.8, 16.2, and 90.0) G of $^{13}C5'$ for $C5^{\bullet}$ for the planar conformation of $C5^{\bullet}$ were found to be very close to experimentally obtained HFCC values (28, 28, and 84) G of $^{13}C5'$ for $C5^{\bullet}$.²⁸ Hence, on the basis of the above-mentioned ESR/ENDOR studies^{28,32,40–42} and theoretical calculation of $C5^{\bullet}$ radical in a B-DNA conformation,⁴³ the lack of an observable $C4'$ - β H in the $C5^{\bullet}$ spectrum found in high molecular weight DNA results in a variety of conformations with the dominant conformations placing the

$C4'$ -H near the nodal plane of the $C5'$ -radical p-orbital. Furthermore, in the ESR spectra in Figure 1A,B, no β -phosphorus coupling is observed. The lack of a β -phosphorus coupling is further elucidated with experiments in section II.

II. Lack of a β -Phosphorus Coupling in $C5^{\bullet}$ —Studies Using Dimethyl Phosphate. It is evident from Figure 1 that the ESR spectrum of $C5^{\bullet}$ found in γ - (low LET) as well as in ion-beam (high LET)-irradiated high molecular weight DNA is an anisotropic ca. 21 G doublet. No evidence for a β -phosphorus atom coupling has been found for $C5^{\bullet}$ either in γ - as well as in ion-beam-irradiated DNA. This lack of an observable β phosphorus coupling in the $C5^{\bullet}$ spectrum found in irradiated DNA is intriguing as the β -phosphorus coupling is dependent on the geometry of the conformation of $C5^{\bullet}$, and our DFT calculations show that it can be large (ca. 40 G) at specific orientations (see the Supporting Information, Figures S1 and S2). Therefore, to elucidate this, we performed ESR studies and DFT calculations using dimethyl phosphate as a model system (Figures 2 and 3 and the Supporting Information, Figures S1 and S2) as it is the simplest structure that mimics the $-\text{CH}_2-\text{O}-\text{PO}_2^--\text{O}-\text{CH}-$ structure of the sugar–phosphate backbone in DNA.

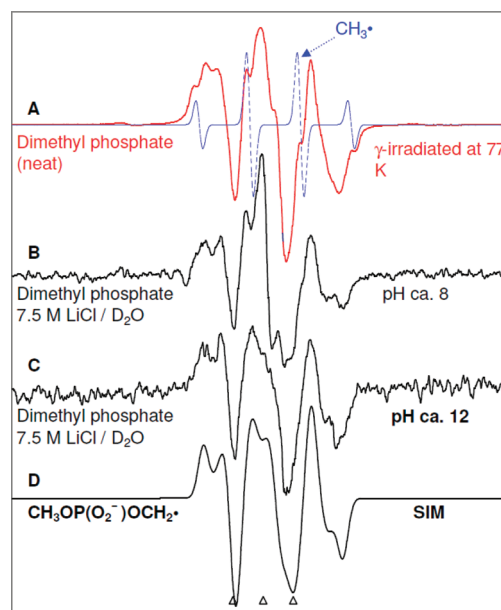


Figure 2. (A) ESR spectrum (red) showing the formation of radiation-induced $\text{CH}_3\text{OP}(\text{O}_2^-)\text{OCH}_2^{\bullet}$ and CH_3^{\bullet} (dotted blue) in γ -irradiated N_2 -saturated neat dimethyl phosphate (200 μL). ESR spectra of radiation-induced $\text{CH}_3\text{OP}(\text{O}_2^-)\text{OCH}_2^{\bullet}$ found in glassy (7.5 M LiCl/D₂O) samples of dimethyl phosphate (B) (5 mg/mL) in the presence of $\text{K}_2\text{S}_2\text{O}_8$ (8 mg/mL) at ca. pH 8 and of (C) dimethyl phosphate (20 mg/mL) in the presence of $\text{K}_2\text{S}_2\text{O}_8$ (8 mg/mL) at ca. pH 12. (D) Simulated spectrum of $\text{CH}_3\text{OP}(\text{O}_2^-)\text{OCH}_2^{\bullet}$ (for simulation parameters, see the text).

It is evident from the spectra in Figure 2A–C that irrespective of pH or concentration of dimethyl phosphate (neat to 20 mg/mL) used in our studies, an anisotropic triplet (1:2:1) is found. It is well-established in the literature that this type of anisotropic 1:2:1 triplet originates due to two α -H couplings of the $-\text{CH}_2^{\bullet}$ group.^{44,45} On this basis, this anisotropic triplet is assigned to two α -H couplings from the CH_2 group in $\text{CH}_3\text{OP}(\text{O}_2^-)\text{OCH}_2^{\bullet}$ (scheme 1). The spectrum of $\text{CH}_3\text{OP}(\text{O}_2^-)\text{OCH}_2^{\bullet}$ has been simulated using the ESR

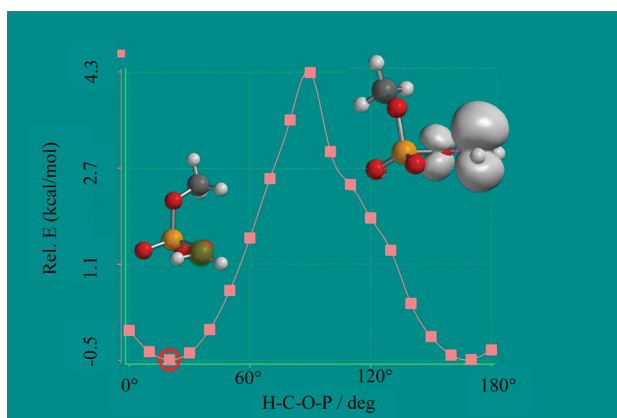


Figure 3. Optimized geometry of the minimum energy conformation (indicated by red circle) and the spin density distribution in the optimized geometry of the minimum energy conformation of $\text{CH}_3\text{OP}(\text{O}_2^-)\text{OCH}_2^\bullet$ in the gas phase obtained by employing the DFT/B3LYP/6-31G(d) method. The potential energy surface of various conformations of $\text{CH}_3\text{OP}(\text{O}_2^-)\text{OCH}_2^\bullet$ was obtained by stepwise (each step = 10°) gradual increase of the dihedral angle P–O–C–H from 0 to 180° in 18 steps.

parameters: 1 αH ($A_{xx}, A_{yy}, A_{zz} = 25.7, 12.64, 19.02, 20.0$ G), 1 αH ($A_{xx}, A_{yy}, A_{zz} = 9.3, 0, 31.3, 20.35$ G), ($g_{xx}, g_{yy}, g_{zz} = 2.0030, 2.0030, 2.0024$) and with a mixed (1:1) Lorentzian/Gaussian line width (4.5, 4.5, 5.5 G). The simulated spectrum (Figure 2D) of $\text{CH}_3\text{OP}(\text{O}_2^-)\text{OCH}_2^\bullet$ matches the experimental spectra in Figure 2A–C quite well.

For glassy samples of dimethyl phosphate at pH values ca. 8 and ca. 12, progressive annealing from 77 to 160 K show loss of intensities of $\text{Cl}_2^{\bullet-}$ line components, but it did not result in any concomitant increase of intensities of the line components belonging to the $\text{CH}_3\text{OP}(\text{O}_2^-)\text{OCH}_2^\bullet$. Thus, our results show that $\text{CH}_3\text{OP}(\text{O}_2^-)\text{OCH}_2^\bullet$ is not formed via one-electron oxidation by $\text{Cl}_2^{\bullet-}$ but is produced via direct radiation-induced ionization followed by deprotonation of the one-electron oxidized species. Furthermore, the spectrum in Figure 2A (red) shows the formation of $\text{CH}_3\text{OP}(\text{O}_2^-)\text{OCH}_2^\bullet$ (predominant) and CH_3^\bullet (small amount, dotted blue). As mentioned earlier,^{25a–d} alkyl radicals have been found in γ -irradiated alkyl phosphates at 77 K; thus, the formation of CH_3^\bullet in γ -irradiated neat dimethyl phosphate at 77 K is expected and is likely a result of a DEA of the C–O bond. We note here that the hydrogen atom abstraction by CH_3^\bullet at 77 K is well established in the literature.^{46,47}

An interesting finding that is evident from the spectra in Figure 2A–C that that irrespective of pH or concentration (neat to 20 mg/mL) of dimethyl phosphate used in our studies, no observable β -hyperfine coupling due to the phosphorus atom in the phosphate group of $\text{CH}_3\text{OP}(\text{O}_2^-)\text{OCH}_2^\bullet$ is found. This clearly shows that in the $\text{CH}_3\text{OP}(\text{O}_2^-)\text{OCH}_2^\bullet$ conformation found in our system, the phosphorus atom is held near the node of the radical site p-orbital. This is supported by theoretical calculations in the gas phase based on the DFT/B3LYP/6-31G(d) method that shows the conformation of $\text{CH}_3\text{OP}(\text{O}_2^-)\text{OCH}_2^\bullet$ with the minimum energy (see Figure 3) has the phosphate P-atom held in the nodal plane of the radical site p-orbital [dihedral angle H–C–O–P (θ) $\approx 0^\circ$]. The theoretically predicted β -P atom HFCC value is -1.4 G, and this HFCC value is too small to be observed experimentally.

We find that for $\text{CH}_3\text{OP}(\text{O}_2^-)\text{OCH}_2^\bullet$ at an H–C–O–P dihedral angle of $\approx 90^\circ$ (Supporting Information, Figures S1 and S2), a large β -P atom hyperfine coupling of ca. 40 G is predicted by the DFT/B3LYP/6-31G(d) method. This conformation of $\text{CH}_3\text{OP}(\text{O}_2^-)\text{OCH}_2^\bullet$ lies over 5 kcal/mol higher in energy than the minimum energy conformation shown in Figure 3, which has no significant phosphorus coupling. These results account for the lack of a β -phosphorus atom hyperfine coupling in $\text{CH}_3\text{OP}(\text{O}_2^-)\text{OCH}_2^\bullet$. Moreover, in the ESR studies of radicals found in the X-ray irradiated (at 10 K) of 5'-dGMP, neither a β -phosphorus coupling nor a significant amount of a phosphate radical was reported.²² The lack of a β -phosphorus coupling is supported by the suggested value (174.41°)^{43a} of the torsion angle (C4'–C5'–O5'–P) for the 5'-phosphate attached to the C5'-radical site, which has the 5'-phosphate is in the radical plane. Therefore, the ESR studies showing formation of $\text{CH}_3\text{OP}(\text{O}_2^-)\text{OCH}_2^\bullet$ in γ -irradiated dimethyl phosphate, DFT calculations of conformational dependence of the phosphorus HFC in $\text{CH}_3\text{OP}(\text{O}_2^-)\text{OCH}_2^\bullet$ along with the likely value of C4'–C5'–O5'–P for the 5'-phosphate attached to the C5'-radical site altogether suggest that the absence of a β -phosphorus atom hyperfine coupling in the C5 $^\bullet$ spectrum obtained from DNA is due to the energetically favorable conformation of C5 $^\bullet$ that holds the phosphorus atom of the 5'-phosphate near the nodal plane of the p-orbital at the C5'-radical site.

CONCLUSIONS

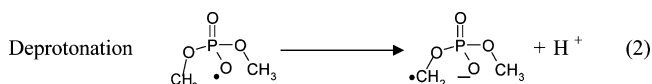
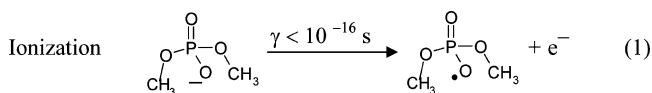
The following salient findings are drawn from the present work.

1. Direct Formation of C5 $^\bullet$ in Monomers and in DNA. Various ESR/ENDOR studies of X-irradiated single crystals of nucleosides and nucleotides show evidence for C5 $^\bullet$ formation.^{22,40–42} For example, radiation-induced formation of C5 $^\bullet$ in addition to C1 $^\bullet$ and C3 $^\bullet$ has been reported in ENDOR studies of X-irradiation at 10 K of single crystals of 5'-dGMP.²² In addition, previous work with irradiated alkyl phosphates,^{25a–d} as well as this work with dimethyl phosphate, support our finding that C5 $^\bullet$ should be directly formed via radiation-induced ionizations in the sugar–phosphate backbone in DNA. Our results for high energy-irradiated DNA do report a slightly higher extent (ca. 40%) of radiation-induced formation of C5 $^\bullet$ in γ -irradiated DNA than in high LET ion-beam-irradiated DNA (ca. 30%). This is likely a result of (a) more C3 $^\bullet$ _{dephos} formation via DEA found in ion-beam-irradiated DNA (compare the spectra in Figure 1A and B) and (b) possibly more fragmentation in the sugar ring of the sugar–phosphate moiety caused by high LET ion-beam irradiation.

2. The Lack of β -Hydrogen and Phosphorus Couplings in C5 $^\bullet$. As predicted by Close⁴² and suggested by Colson and Sevilla,⁴³ no observable β H-atom or β -P atom hyperfine coupling are expected for C5 $^\bullet$ in DNA; these predictions are confirmed by the ESR spectrum of radiation-induced C5 $^\bullet$ in DNA (Figure 1) with no observable β H-atom or β -P atom hyperfine coupling. In addition, the combination of ESR and theoretical work on the model system of the DNA sugar–phosphate backbone–dimethyl phosphate also shows that the phosphorus atom of the phosphate group lies near the nodal plane of the radical site p-orbital in its equilibrium position and results in no β -phosphorus coupling.

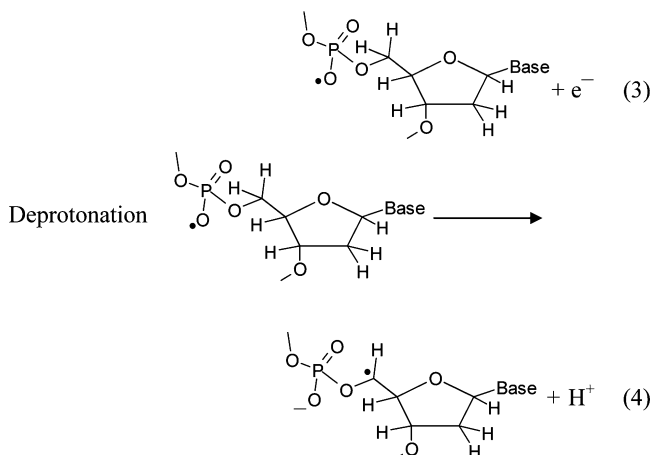
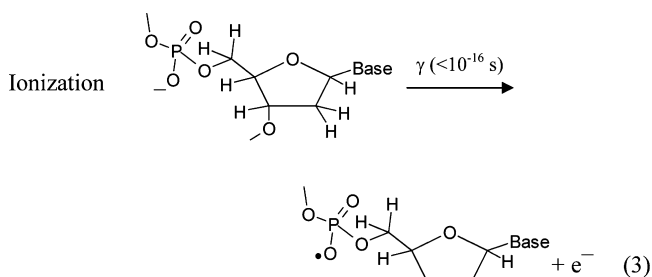
3. Mechanism of Radiation-Induced C5 $^\bullet$ Formation in DNA Based on the Mechanism of $\text{CH}_3\text{OP}(\text{O}_2^-)\text{OCH}_2^\bullet$ Formation in Irradiated Dimethyl Phosphate. In dimethyl phosphate, one-electron oxidation at phosphate by high-energy

radiation results in ionization in proportion to the number of valence electrons. Thus, the formation of $\text{CH}_3\text{OP}(\text{O}_2^-)\text{OCH}_2^\bullet$ in dimethyl phosphate by high-energy radiation involves instantaneous electron loss ($<10^{-16}$ s) from radiation-induced ionization (reaction 1)^{1,8–13} followed by fast deprotonation (reaction 2) of the transient one-electron oxidized intermediate.



Thus, steps 1 and 2 are the expected lowest energy pathway for formation of $\text{CH}_3\text{OP}(\text{O}_2^-)\text{OCH}_2^\bullet$ from irradiated dimethyl phosphate in rigid (glassy) systems at 77 K.

On this basis, the radiation-induced formation of C5^\bullet via direct ionization in the sugar–phosphate backbone of DNA would follow the radiation-induced ionization (reaction 3) and deprotonation (reaction 4) pathways:



It is evident from steps 1 and 3 that as a result of radiation-induced ionization of the phosphate moiety, the charge of the phosphate is lost. After deprotonation (steps 2 and 4), the charge on the phosphate moiety is reinstated to the original charge state. The restitution of charge after an ionization event is a highly favorable process at 77 K.^{50,51} Thus, there are two competing processes for the holes that are formed in the sugar–phosphate backbone after direct ionization: deprotonation at sugar CH sites, for example, $\text{C5}'$, or transfer of the radiation-produced holes to the DNA base moieties. This work in combination with the ESR studies in the range 4–77 K^{8–13,48,49} clearly establishes that the relative rate of deprotonation at the C–H sites in the sugar moiety after radiation-induced ionization of the sugar–phosphate backbone is competitive with that of hole transfer from the ionized sugar–phosphate backbone to the bases at 77 K. ESR studies at 77 K have shown that the extent of stabilized holes on the bases (i.e., one-electron oxidized bases) increases from the expected value 43% (based on valence electrons) to ca. 77% at 77 K. Hence, a majority of the holes from the ionized sugar–phosphate backbone do transfer to the bases at 77 K. However,

our ESR work at 77 K establishes that deprotonation on sugar accounts for the remaining 23% of the original radiation-produced holes due to ionization on the sugar–phosphate backbone. We note here that product analyses studies for unaltered base release (a monitor of sugar radical formation) from irradiated DNA at 77 K also suggested partial transfer of holes to the bases after ionization of the sugar–phosphate DNA backbone.^{14,15} Thus, the competition between deprotonation and hole transfer processes is well supported by both free radical and product studies.

■ ASSOCIATED CONTENT

Supporting Information

Figure S1 showing the optimized geometry of the highest energy conformation of $\text{CH}_3\text{OP}(\text{O}_2^-)\text{OCH}_2^\bullet$ and Figure S2 representing the spin density distribution in the optimized geometry of the highest energy conformation of $\text{CH}_3\text{OP}(\text{O}_2^-)\text{OCH}_2^\bullet$. This material is available free of charge via the Internet at <http://pubs.acs.org>.

■ AUTHOR INFORMATION

Corresponding Author

*Tel: 001 248 370 2328. Fax: 001 248 370 2321. E-mail: sevilla@oakland.edu.

Notes

The authors declare no competing financial interest.

■ ACKNOWLEDGMENTS

We thank the National Cancer Institute of the National Institutes of Health (Grant RO1CA45424) for support. We also thank and gratefully acknowledge Dr. Reginald Ronningen, Dr. R. Anantaraman, and the laboratory staff of the National Superconducting Cyclotron Laboratory at Michigan State University for their assistance with the heavy ion-beam irradiations.

■ REFERENCES

- (1) von Sonntag, C. *Free-Radical-Induced DNA Damage and Its Repair*; Springer-Verlag: Berlin, Heidelberg, 2006; pp 335–447.
- (2) Ward, J. F. *Cold Spring Harb. Symp. Quant. Biol.* **2000**, *65*, 377–382.
- (3) (a) Pogozelski, W. K.; Tullius, T. D. *Chem. Rev.* **1998**, *98*, 1089–1108. (b) Greenberg, M. M. *Org. Biomol. Chem.* **2007**, *5*, 18–30.
- (4) Chan, W.; Chen, B.; Wang, L.; Taghizadeh, K.; Demott, M. S.; Dedon, P. C. *J. Am. Chem. Soc.* **2010**, *132*, 6145–6153.
- (5) Chatgililoglu, C.; Ferreri, C.; Terzidis, M. A. *Chem. Soc. Rev.* **2011**, *40*, 1368–1382.
- (6) (a) Peng, X.; Hong, I. S.; Seidman, M. M.; Greenberg, M. M. *J. Am. Chem. Soc.* **2008**, *130*, 10299–10306. (b) Peng, X.; Ghosh, A. K.; Van Houten, B.; Greenberg, M. M. *Biochemistry* **2010**, *49*, 11–19.
- (c) Jacobs, A. C.; Resendiz, M. J.; Greenberg, M. M. *J. Am. Chem. Soc.* **2011**, *133*, 5152–5159.
- (7) (a) Goodhead, D. T. *Int. J. Radiat. Biol.* **1994**, *65*, 7–17. (b) Nikjoo, H.; Uehara, S.; Wilson, W. E.; Hoshi, M.; Goodhead, D. T. *Int. J. Radiat. Biol.* **1998**, *73*, 355–364.
- (8) Becker, D.; Adhikary, A.; Sevilla, M. D. In *Charge Migration in DNA: Physics, Chemistry and Biology Perspectives*; Chakraborty, T., Ed.; Springer-Verlag: Berlin, Heidelberg, NY, 2007; pp 139–175.
- (9) Becker, D.; Adhikary, A.; Sevilla, M. D. In *Recent Trends in Radiation Chemistry*; Rao, B. S. M., Wishart, J., Eds.; World Scientific Publishing Co.: Singapore, New Jersey, London, 2010; pp 509–542.
- (10) (a) Becker, D.; Adhikary, A.; Sevilla, M. D. In *Charged Particle and Photon Interactions with Matter—Recent Advances, Applications, and Interfaces*; Hatano, Y., Katsumura, Y., Mozumder, A., Eds.; CRC Press,

- Taylor & Francis Group: Boca Raton, London, NY, 2010; pp 503–541. (b) Adhikary, A.; Kumar, A.; Becker, D.; Sevilla, M. D. In *Encyclopedia of Radicals in Chemistry, Biology and Materials*; Chatgililoglu, C., Struder, A., Eds.; John Wiley & Sons Ltd.: Chichester, United Kingdom, 2012; pp 1371–1396.
- (11) Bernhard, W. A.; Close, D. M. In *Charged Particle and Photon Interactions with Matter Chemical, Physicochemical and Biological Consequences with Applications*; Mozumdar, A., Hatano, Y., Eds.; Marcel Dekkar, Inc.: New York, Basel, 2004; pp 431–470.
- (12) Bernhard, W. A. In *Radical and Radical Ion Reactivity in Nucleic Acid Chemistry*; Greenberg, M. M., Ed.; John Wiley & Sons, Inc.: New Jersey, 2009; pp 41–68.
- (13) Close, D. M. In *Radiation-Induced Molecular Phenomena in Nucleic Acids: A Comprehensive Theoretical and Experimental Analysis*; Shukla, M. K., Leszczynski, J., Eds.; Springer-Verlag: Berlin, Heidelberg, NY, 2008; 493–529.
- (14) Swarts, S. G.; Sevilla, M. D.; Becker, D.; Tokar, C. J.; Wheeler, K. T. *Radiat. Res.* **1992**, *129*, 333–344.
- (15) Swarts, S. G.; Becker, D.; Sevilla, M. D.; Wheeler, K. T. *Radiat. Res.* **1996**, *145*, 304–314.
- (16) Shukla, L. I.; Pazdro, R.; Becker, D.; Sevilla, M. D. *Radiat. Res.* **2005**, *163*, 591–602.
- (17) Becker, D.; Razskazovskii, Y.; Callaghan, M. U.; Sevilla, M. D. *Radiat. Res.* **1996**, *146*, 361–368.
- (18) Becker, D.; Bryant-Friedrich, A.; Trzasko, C.; Sevilla, M. D. *Radiat. Res.* **2003**, *160*, 174–185.
- (19) Fernando, H.; Papadantonakis, G. A.; Kim, N. S.; LeBreton, P. R. *Proc. Natl. Acad. Sci. U.S.A.* **1998**, *95*, 5550–5555.
- (20) Hou, R.; Gu, J.; Xie, Y.; Yi, X.; Schaefer, H. F. *J. Phys. Chem. B* **2005**, *109*, 22053.
- (21) Close, D. M. *J. Phys. Chem. A* **2008**, *112*, 8411–8417.
- (22) Hole, E. O.; Nelson, W. H.; Sagstuen, E.; Close, D. M. *Radiat. Res.* **1992**, *129*, 119–138.
- (23) Wang, W.; Sevilla, M. D. *Int. J. Radiat. Biol.* **1994**, *66*, 683–695.
- (24) Malone, M. E.; Cullis, P. M.; Symons, M. C. R.; Parker, A. W. *J. Phys. Chem.* **1995**, *99*, 9299–9308.
- (25) (a) Bernhard, W. A.; Ezra, F. S. *J. Chem. Phys.* **1974**, *60*, 1707–1710. (b) Ezra, F. S.; Bernhard, W. A. *Radiat. Res.* **1974**, *60*, 350–354. (c) Nelson, D.; Symons, M. C. R. *J. Chem. Soc. Perkin Trans. II* **1977**, 286–293. (d) Sanderud, A.; Sagstuen, E. *J. Chem. Soc. Faraday Trans.* **1996**, *92*, 995–999. (e) Shaw, A. A.; Cadet, J. *Int. J. Radiat. Biol.* **1988**, *54*, 987–997. (f) Shaw, A. A.; Cadet, J. *Int. J. Radiat. Biol.* **1996**, *70*, 1–6.
- (26) (a) Shukla, L. I.; Adhikary, A.; Pazdro, R.; Becker, D.; Sevilla, M. D. *Nucleic Acids Res.* **2004**, *32*, 6565–6574. (b) Shukla, L. I.; Adhikary, A.; Pazdro, R.; Becker, D.; Sevilla, M. D. *Nucleic Acids Res.* **2007**, *35*, 2460–2461.
- (27) Adhikary, A.; Malkhasian, A. Y. S.; Collins, S.; Koppen, J.; Becker, D.; Sevilla, M. D. *Nucleic Acids Res.* **2005**, *33*, 5553–5564.
- (28) Adhikary, A.; Becker, D.; Collins, S.; Koppen, J.; Sevilla, M. D. *Nucleic Acids Res.* **2006**, *34*, 1501–1511.
- (29) (a) Adhikary, A.; Kumar, A.; Sevilla, M. D. *Radiat. Res.* **2006**, *165*, 479–484. (b) Adhikary, A.; Collins, S.; Khanduri, D.; Sevilla, M. D. *J. Phys. Chem. B* **2007**, *111*, 7415–7421.
- (30) Adhikary, A.; Kumar, A.; Becker, D.; Sevilla, M. D. *J. Phys. Chem. B* **2006**, *110*, 24170–24180.
- (31) Adhikary, A.; Kumar, A.; Khanduri, D.; Sevilla, M. D. *J. Am. Chem. Soc.* **2008**, *130*, 10282–10292.
- (32) Adhikary, A.; Khanduri, D.; Kumar, A.; Sevilla, M. D. *J. Phys. Chem. B* **2008**, *112*, 15844–15855.
- (33) Adhikary, A.; Khanduri, D.; Sevilla, M. D. *J. Am. Chem. Soc.* **2009**, *131*, 8614–8619.
- (34) Adhikary, A.; Kumar, A.; Munafo, S. A.; Khanduri, D.; Sevilla, M. D. *J. Phys. Chem. Chem. Phys.* **2010**, *12*, 5353–5368.
- (35) Khanduri, D.; Adhikary, A.; Sevilla, M. D. *J. Am. Chem. Soc.* **2011**, *133*, 4527–4537.
- (36) (a) SPARTAN, version 10; Wavefunction, Inc.: Irvine, CA, 2010. (b) Frisch, M. J.; Trucks, G. W.; Schlegel, H. B.; Scuseria, G. E.; Robb, M. A.; Cheeseman, J. R.; Scalmani, G.; Barone, V.; Mennucci, B.; Petersson, G. A.; Nakatsuji, H.; Caricato, M.; Li, X.; Hratchian, H. P.; Izmaylov, A. F.; Bloino, J.; Zheng, G.; Sonnenberg, J. L.; Hada, M.; Ehara, M.; Toyota, K.; Fukuda, R.; Hasegawa, J.; Ishida, M.; Nakajima, T.; Honda, Y.; Kitao, O.; Nakai, H.; Vreven, T.; Montgomery, J. A., Jr.; Peralta, J. E.; Ogliaro, F.; Bearpark, M.; Heyd, J. J.; Brothers, E.; Kudin, K. N.; Staroverov, V. N.; Kobayashi, R.; Normand, J.; Raghavachari, K.; Rendell, A.; Burant, J. C.; Iyengar, S. S.; Tomasi, J.; Cossi, M.; Rega, N.; Millam, J. M.; Klene, M.; Knox, J. E.; Cross, J. B.; Bakken, V.; Adamo, C.; Jaramillo, J.; Gomperts, R.; Stratmann, R. E.; Yazyev, O.; Austin, A. J.; Cammi, R.; Pomelli, C.; Ochterski, J. W.; Martin, R. L.; Morokuma, K.; Zakrzewski, V. G.; Voth, G. A.; Salvador, P.; Dannenberg, J. J.; Dapprich, S.; Daniels, A. D.; Farkas, O.; Foresman, J. B.; Ortiz, J. V.; Cioslowski, J.; Fox, D. J. *Gaussian 09*; Gaussian, Inc.: Wallingford, CT, 2009.
- (37) Hermosilla, L.; Calle, P.; García de la Vega, J. M.; Sieiro, C. *J. Phys. Chem. A* **2005**, *109*, 1114–1124.
- (38) Hermosilla, L.; Calle, P.; García de la Vega, J. M.; Sieiro, C. *J. Phys. Chem. A* **2006**, *110*, 13600–13608.
- (39) Close, D. M. *J. Phys. Chem. A* **2010**, *114*, 1860–1187.
- (40) Close, D. M.; Nelson, W. H.; Sagstuen, E.; Hole, E. O. *Radiat. Res.* **1994**, *137*, 300–309.
- (41) Alexander, C., Jr.; Franklin, C. E. *J. Chem. Phys.* **1971**, *54*, 1909–1913.
- (42) Close, D. M. *Radiat. Res.* **1997**, *147*, 663–673.
- (43) (a) Colson, A.-O.; Sevilla, M. D. *J. Phys. Chem.* **1995**, *99*, 3867–3874. (b) Colson, A.-O.; Sevilla, M. D. *Int. J. Radiat. Biol.* **1995**, *67*, 627–645.
- (44) Symons, M. C. R. In *Advances in Physical Organic Chemistry*; Gold, V., Ed.; Academic Press: New York, 1963; Vol. 1, pp 284–363.
- (45) Sullivan, P. J., Sr; Koski, W. S. *J. Am. Chem. Soc.* **1963**, *85*, 384–387.
- (46) Sprague, E. D. *J. Phys. Chem.* **1973**, *77*, 2066–2070.
- (47) Campion, A.; Williams, F. *J. Am. Chem. Soc.* **1972**, *94*, 7633–7637.
- (48) (a) Spalletta, R. A.; Bernhard, W. A. *Radiat. Res.* **1992**, *130*, 7–14. (b) Weiland, B.; Hüttermann, J. *Int. J. Radiat. Biol.* **1998**, *74*, 341–358. (c) Weiland, B.; Hüttermann, J. *Int. J. Radiat. Biol.* **1999**, *75*, 1169–1175. (d) Debije, M. G.; Bernhard, W. A. *J. Phys. Chem. B* **2000**, *104*, 7845–7851.
- (49) Long Range Charge Transfer in DNA. I and II, *Topics in Current Chemistry*; Schuster, G. B., Ed.; Springer-Verlag: Berlin, Heidelberg, 2004.
- (50) Nelson, W. H.; Sagstuen, E.; Hole, E. O.; Close, D. M. *Radiat. Res.* **1998**, *149*, 75–86.
- (51) Bernhard, W. A.; Barnes, J.; Mercer, K. R.; Mroczka, N. *Radiat. Res.* **1994**, *140*, 199–214.